Chemical Engineering Journal 97 (2004) 141–149

Chemical Engineering Journal

www.elsevier.com/locate/cej

Mass transfer enhancement at vibrating electrodes

H. Gomaa [a,*], A.M. Al Taweel [a], J. Landau [b]

[a] *Chemical Engineering Department, Dalhousie University, Halifax, NS, Canada B3J 2X4*
[b] *University of New Brunswick, Fredericton, NB, Canada*

Received 15 February 2003; accepted 14 May 2003

Abstract

The potential for reducing mass transfer limitation at vertical electrodes through the application of vibrations was investigated using the limiting current technique. A wide range of experimental conditions was used (frequencies of 0–25 Hz, amplitudes of 0–20 mm, and electrode heights of 3–130 mm) and both the instantaneous and the average mass transfer rates were measured.

Up to 23-fold increase in the average rate of mass transfer was achieved by vibrating the flat vertical plates parallel to their surfaces. The results obtained were well correlated using a quasi-steady state approach for mass transfer across a boundary layer over a flat plate where the average vibrational velocity over a cycle was used as a characteristic velocity.

Keywords: Mass transfer; Electrodes; Vibration; Enhancement; Process intensification

1. Introduction

The application of vibrations, sonics, and ultrasonics has been recognized as an effective process intensification (PI) technique that enhances mass and heat transfer rates, and improves both process productivity and product quality [1–10]. Their use in electrochemical processing [11–20] has been of particular interest due to their ability to reduce diffusion controlled processes which limits both the maximum allowable current density and the cell energy efficiency. This is particularly true for dilute solutions where the low concentration of the active species necessitates the use of electrodes with large surface area, or increased fluid pumping/recirculation, approaches which result in higher capital and processing costs. The use of vibration minimizes such needs by intensifying mass transfer at the solid–liquid interface which, in turn, reduces the required processing size and enhances the process safety.

Controlled vibrations technique has been applied in many electrochemical processes, and several patents have been granted for different arrangement and approaches for its use. These includes electroplating, production of fine metallic powders, metal recovery from bio-leaching solutions, and treatment of wastewater effluents [4,12,17]. It was also found to be beneficial in conducting controlled electro-organic synthesis [21,22], and more recently in the manufacture of Printed Wiring Board where electroplating is re-emerging of as the preferred technology for producing “Sub-Micron Multi-Level Metallization” in ultra large scale integration [23–25].

In all of the above mentioned applications, generating of an oscillatory field at the solid–liquid interface is achieved by vibrating either the solid surface or the fluid surrounding it. Although both approaches achieve the same objective, the former is more energy efficient since the energy dissipation there is mainly focused in the boundary layer adjacent to the solid–liquid interface rather than in the bulk of the fluid medium. When the power needed to vibrate the electrode was taken into consideration, Al Taweel et al. [16] found that both amplitude and frequency have almost equal effect on the enhancement obtained per unit power consumed.

Although the influence of hydrodynamics on the transport mechanisms in electrochemical cells has been the subject of many scientific and industrial investigations [26,27], the situation is different for cells where vibration is used for mass transfer enhancement, and some deficiency still exist in understanding the contribution of the different mechanisms to the overall enhancement factor. For example, and as shown by Al Taweel and co-workers [9,17] and Drummond and Lyman [28], mass transfer enhancement due to the formation of turbulent eddies is significantly different from that caused by acoustic streaming and boundary layer thinning, and the

* Corresponding author. Present address: Chemical Engineering Department, Dalhousie University, P.O. Box 1000, Halifax, NS, Canada B3J 2X4. Mail address: P.O. Box 2103, Port Elgin, Ont., Canada.
Fax: +1-519-797-1956.
E-mail address: gomaah@bmts.com (H. Gomaa).

1385-8947/$ – see front matter © 2003 Elsevier B.V. All rights reserved.
doi:10.1016/S1385-8947(03)00152-9

Nomenclature

a	electrode active surface area (mm^2)
A	amplitude of electrode vibration (mm)
C_B	bulk concentration of the ferri-ferrocyanide (mol/mm^3)
ΔC	concentration difference (mol/mm^3)
D	diffusion coefficient (mm^2/s)
E	mass transfer enhancement factor
f	frequency of electrode vibration (Hz)
F	Faraday's constant (C/eq.)
G	acceleration of gravity (cm/s^2)
Gr	Grashof number ($\alpha \Delta C g L^3/\nu^2$)
I_L	limiting current (C/s)
K_{nc}	free convective mass transfer coefficient (mm/s)
K_v	vibrational mass transfer coefficient (mm/s)
L	length of electrode active area (mm)
n	number of electrons transferred in the electrode reaction
Re_v	vibrational Reynolds number
$S(t)$	shear rate at the solid–liquid interface (s^{-1})
Sc	Schmidt number (ν/D)
Sh_{nc}	natural convection Sherwood number ($k_{nc}L/D$)
Sh_v	vibrational Sherwood number (k_vL/D)

Greek letters

α	concentration coefficient of volumetric expansion (mm^3/mol)
ν	kinematic viscosity (mm^2/s)
ω	circular frequency of vibration, $2\pi F$ (s^{-1})

Subscripts

nc	natural convection
v	vibrational

parameters affecting the two approaches are also significantly different. This should be taken into consideration while interpreting and scaling up of the results, a task that could be extremely complex if more than one mechanism exists. The lack of proper understanding of such an issue resulted in large disagreement between the various investigators, such as the case when comparing results for traverse vibrations [29], with those in which the electrodes were vibrated parallel to their surfaces [30,17,18]. Proper understanding of the enhancement mechanism is necessary in order to allow for the development of proper scale-up methodologies and for achieving the full potential of using controlled vibration as a process intensification tool.

The objective of this work is to address the above deficiency by attempting to investigate the contribution of a specific mass transfer mechanism to the overall enhancement factor with minimum interaction or presence of the other mechanisms. To achieve that, the effect of longitudinal vibration on the mass transfer enhancement was investigated using specially-designed flat electrodes that eliminate acoustic streaming, the formation of turbulent eddies, and minimizes the effects of the plate's leading edge. This allows for better understanding of the contribution of shear reversal to the mass transfer enhancement at flat surfaces in absence of other mechanisms related to bodies of revolutions, or those related to the formation and impingement of turbulent eddies.

2. Experimental

Because of its accuracy and relative simplicity, the mass transfer coefficient was measured using the limiting current technique. The experimental set-up used is schematically depicted in Fig. 1. It consists of three main subsections: the electrolytic cell, the vibration inducing system, and the power supply/current-measurement system. Measurements were conducted in a 30 l rectangular Plexiglas tank (400 mm × 250 mm × 345 mm) filled with 0.01 M potassium ferri-ferrocyanide in a 2 M sodium hydroxide solution. This system was selected because of its fast electron transfer kinetics and the consequent ability to monitor very rapid variations in mass transfer rates, a situation that is expected to be of significant importance in the present investigation. Furthermore, this system has the advantage of maintaining the concentration of both chemicals constant throughout the experiment since ferricyanide is reduced to ferrocyanide at the cathode surface while the reverse reaction occurs at the anode surface.

The cell was covered with black plastic film to protect against photochemical decomposition of the electrolyte. The container cover was designed to hold a reference probe, a nitrogen sparger, a thermometer, and was equipped with a special opening to allow for the free movement of the working electrode. To reduce the effect of dissolved oxygen, freshly prepared solutions were purged with oxygen-free nitrogen for 12 h before its use. Moreover, nitrogen purge was also applied for half an hour before the start of any experiment to de-oxygenate the headspace. To ensure chemical composition stability, a new solution was prepared weekly, and the concentration was checked as per standard procedures at the beginning and at the end of each week.

A 300 mm × 425 mm nickel sheet was attached to cell wall opposite the electrode and served as a stationary anode. Eight active cathodes (varying in height between 3 and 130 mm) were made out of nickel sheet (30 mm wide) and embedded into a 50 mm Plexiglas carrier plate in a fashion that ensured the absence of any surface deformity. The leading edge of the Plexiglas carrier plate was tapered to eliminate streaming and eddy generation at the vibrating leading edge. The effect of this interference on the measurements was further minimized by placing the active cathode surface at least 50 mm away from the leading edge. Two perpendicular ribs were also added to the back of the carrier plate in order to eliminate the onset of lateral vibrations, a factor

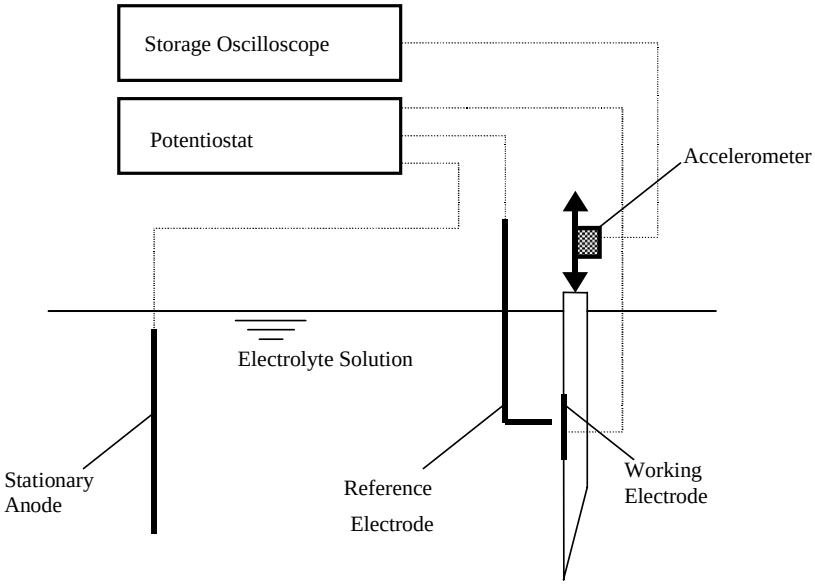

Fig. 1. Schematic diagram of the experimental set-up.

which is suspected to have interfered with the results of Al Taweel and co-workers [16,17].

Princeton Applied Research Corp. potentiostat was used to set and maintain the potential difference between the cathode and the solution. The counter electrode was made of a nickel rod located at the mid-height of the cathode. Due to the high conductivity of the electrolyte, changing the probe's position was found to have no effect on the current density. The response time of the instrument (<1 ms) is much smaller than that of the vibrational motion, thereby allowing for accurate measurement of the transient current density with time. The instantaneous current signal was recorded. A high frequency filter was used to eliminate high-frequency signal noise while the high precision ammeter included in the potentiostat measured the average current.

The Plexiglas carrier plates, in which the electrodes are embedded, were vibrated in the vertical direction using an adjustable eccentric driven by a variable speed motor. This arrangement allowed for a wide range of vibratory conditions to be imparted to the electrodes ($f = 0$–25 Hz, and $A = 0$–20 mm). This motion was monitored using an accelerometer attached to the drive shaft and the resulting signal was stored on the same storage system used for recording the instantaneous value of the limiting current. Both the limiting current and the velocity signals were simultaneously displayed on the same window. This allowed for the accurate determination of the shape and magnitude of instantaneous vibrational frequency and the corresponding limiting current.

2.1. Experimental procedure

In order to enhance the reproducibility of results, it is necessary to maintain the surface conditions of the electrode as uniform as possible. Consequently, for each experimental run, the cathode surface was polished with increasingly fine grades of emery paper/paste and treated cathodically in a 5% NaOH solution at a current density of 20 mA/cm^2 for about 15 min in order to allow for hydrogen evolution and surface activation. The cathode was then rinsed with distilled water and placed in the cell. Similarly, the anode was cleaned with fine emery paper and rinsed with distilled water before placing it into the cell. This resulted in decreasing the reproducibility error to within ±3%.

Experiments were conducted at 25±0.5 °C using a potentiostatic approach (at a cell potential of 500 mV). This potential lies approximately at the midpoint of the plateau zone of the current–voltage curve. For each electrode height the steady-state limiting current was measured under stationary electrode conditions to determine the free convective mass transfer coefficient for that particular electrode height. The effect of vibration on the limiting current was then measured for a range of vibrational frequencies at particular amplitudes.

2.2. Mass transfer calculations

The electrode chemical reactions taking place in the above-mentioned system is such that ferricyanide is reduced to ferrocyanide at the cathode surface while the reverse reaction occurs at the anode surface. At the limiting current conditions, the concentration of the ferricyanide is reduced to virtually zero at the cathode surface. The mass transfer coefficient, k, can, therefore, be calculated from the following equation,

$$k = \frac{I_L}{anFC_b} \quad (1)$$

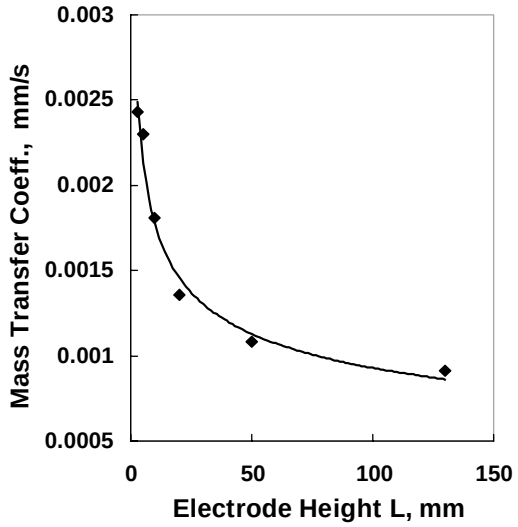

Fig. 2. Mass transfer at stationary vertical electrodes.

3. Results and discussion

Generally speaking, the rate of mass transfer at a stationary vertical electrode surface is controlled by natural convection. To check the accuracy of the experimental set-up, the free convective mass transfer for stationary non-vibrating electrodes was measured and compared with long standing correlations reported in the literature. Under those conditions, the difference in density between the electrolyte near the cathode surface and that in the bulk induces natural convection. As can be seen from Fig. 2, the results obtained agree within ±4% with the laminar free convective mass transfer data for vertical surfaces reported by Fouad and Gouda [31], after applying the corrections proposed by Selman and Newman [33] and Taylor and Hanratty [32], which leads to the well known equation for free convection at vertical electrodes, given by,

$$Sh_n = 0.67(GrSc)^{0.25} \quad (2)$$

3.1. Transient behaviour of the limiting current

The rate of mass transfer at the surface of stationary vertical electrodes is controlled by diffusion through a natural convection boundary layer created by the density difference between the reactants and products at the surface of the electrode. When the electrodes were vibrated, the average current density was found to increase substantially as either the frequency or amplitude is increased. Its instantaneous value exhibited a definite oscillatory component (ac) superimposed on a much larger pseudo-steady one (dc). Furthermore, the magnitude and shape of the ac component was found to be dependent on the electrode height as well as the vibrational parameters.

The magnitude of the ac component was found to be much smaller than the dc value within the range of experimental conditions investigated. This is in qualitative agreement with previously reported heat and mass transfer experiments [10,18,34], which suggest that under pseudo-steady state conditions, the thickness of the diffusion layer, and consequently the mass transfer flux, undergo relatively little changes throughout the vibratory cycle and does not follow the oscillatory velocity which periodically approaches zero and reverses direction. The interferograms of the heat transfer boundary layer at a longitudinally vibrating vertical plate obtained by Prasad and Ramanathan [35] confirmed the above observation and showed that the boundary layer had an almost steady thickness that did not significantly change with time throughout the vibratory cycle.

The shape of the ac mass transfer component, which is always positive, behaved as a complex composite signal of two sub-harmonics with characteristic frequencies f and $2f$ that varied in magnitude and interaction depending on the electrode height and vibrational parameters (Fig. 3). Such an observation also confirms the previously mentioned fact that the instantaneous mass flux does not follow the surface velocity, which would have resulted in harmonic mass transfer with a characteristic frequency of $2f$. This is also consistent with the results of Liu et al. [18], who also obtained similar shapes of the ac component for mass transfer at vibrating electrodes.

The above authors, however, attributed the phenomenon to the location of the electrode's active area in relation to the leading edge of the reciprocating surface. They thus reported that the ac current component is dominated by a harmonic of frequency $1f$ when the electrode active area was located at the leading edge of the reciprocating plate but is dominated by a harmonic of $2f$ frequency in cases where the active area was placed far away from the leading edge. Their interpretation was based on the results of Watkins and Herron [34] where it was shown that the velocity gradient at the leading edge of an oscillating surface is infinite but decreases sharply with increasing distance from the leading edge until it reaches a constant value identical to that of an infinite plate oscillating at the same frequency and amplitude, i.e. Stokes flows, at a distance A from the leading edge. The results obtained in the present investigation do not support the explanation proposed by Liu et al. since, in all of our experiments, the distance between the leading edge and the electrode active area was always greater than $2A$, and the presence of the first or second harmonics depended only on the electrode height and its vibrational parameters.

In light of the above discussion, it seems that such complex behaviour can be best explained in terms of the interaction between two mass transfer mechanisms. The first being a vibrationally-enhanced steady convective mass transfer mechanism that does not change direction or magnitude during the electrode oscillatory cycle, while the second is an oscillatory one that reverses direction during the cycle. The relative magnitude and contribution of each mechanism varies with the electrode height and vibrational parameters. At this point, no models that are capable of predicting the

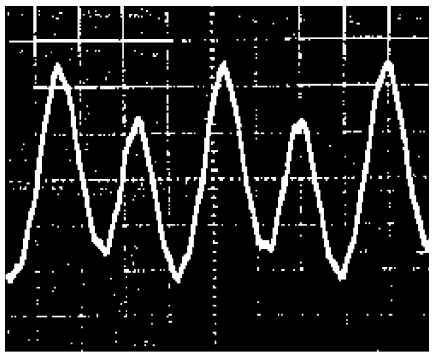
(a)

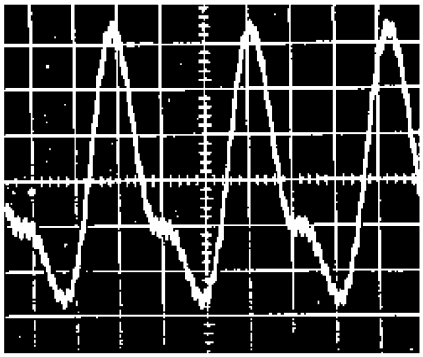
(b)

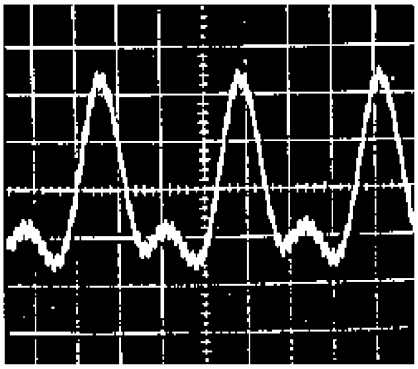
(c)

Fig. 3. Temporal variation in limiting current. (a) $f = 5$ Hz, $A = 20$ mm, $L = 3$ mm; (b) $f = 3$ Hz, $A = 3$ mm, $L = 5$ mm; (c) $f = 3$ Hz, $A = 3$ mm, $L = 3$ mm.

relative contribution and interaction of each mechanism on the overall mass transfer value were found.

3.2. Data analysis

Figs. 4 and 5 show the effect of vibrational frequency and amplitude on the average vibrational mass transfer coefficient (k_v) for different electrode heights. As can be seen from those figures, the average mass transfer coefficient increases with increasing either the frequency or the amplitude of vibration with the extent of enhancement being most pronounced at small electrode heights. The effect of the vibrational amplitude and frequency on the value of the average mass transfer coefficient was found to be almost the same.

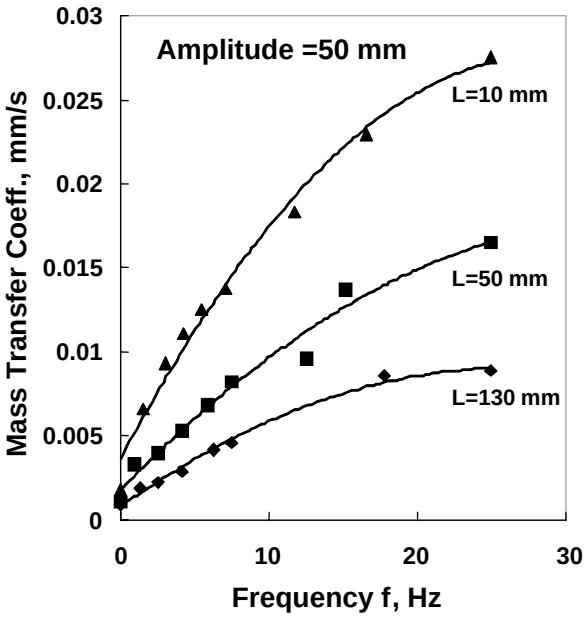

Fig. 4. Effect of vibrational frequency on the average mass transfer coefficient ($A = 5$ mm).

To account for the effect of natural convection in mixed forced and natural convection, Acrivos [36] indicated that the ratio ($Gr/Re^2Sc^{1/3}$) is a critical parameter, and that forced convection prevails if this ratio is <0.1. Prasad and Ramanathan [35] showed that the criterion set forth by Acrivos is also valid for oscillatory flow conditions if the Reynolds number is defined as the vibrational Reynolds number Re_v,

$$Re_v = \frac{A\omega L}{\nu} \tag{3}$$

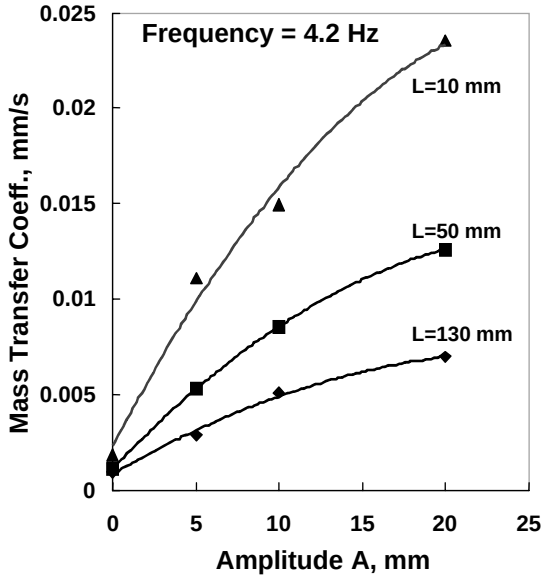

Fig. 5. Effect of vibrational amplitude on the average mass transfer coefficient ($f = 4.2$ Hz).

In almost all of our experiments, the ratio $Gr/Re_v^2Sc^{1/3}$ was <0.1, therefore, it is reasonable to correlate the data using a forced convection approach. Previous investigators proposed several models to account for the increased average transfer rates between fluids and solid surfaces under oscillatory flow conditions. The simplest is the Stretched-Film (STFLM) concept [17], which attributes the mass transfer enhancement to the formation of an effective film area equivalent to the total area swept out during each cycle. This model is expected to apply when high-frequency low-amplitude vibrations are applied. Under those conditions, the mass transfer can be correlated using an empirically determined constant λ by,

$$Sh_v = Sh_{nc}\left[1 + \lambda Re_v\left(1 + \frac{2A}{L}\right)^2\right] \quad (4)$$

Another approach, usually referred to as the boundary layer thinning (BLTH), is based on the analogy between mass and momentum transfer, which leads to the assumption that the diffusion boundary layer thickness will be reduced in the presence of oscillatory motion in a manner similar to a Stokes layer [37]. This approach yields,

$$Sh_v = \lambda' Re_v^{1/2}\left(\frac{L}{A}\right)^{1/2} \quad (5)$$

The third approach is based the boundary layer (BL) theory, which under quasi-steady-state conditions and high values of *Sc* numbers, yields the one-third power law,

$$Sh(t) = 0.808\left\{\frac{S(t)L^2}{D}\right\}^{1/3} \quad (6)$$

where $S(t)$ is the shear rate at the solid–liquid interface. Al Taweel and Ismail [17] used Eq. (6), and by assuming Stokes flow conditions to apply, they obtained the following expression for the time average mass transfer coefficient,

$$Sh_v = 0.665 Re^{1/2}Sc^{1/3}\left(\frac{A}{L}\right)^{1/6} \quad (7)$$

This modelling approach applies only for infinitely long electrodes. A better description of the hydrodynamic conditions may be achieved by assuming that Blasius flow prevails. Under such conditions, Eq. (6) yields the well known equation for mass transfer across a boundary layer over a flat plate given by [38],

$$Sh_v = 0.678 Re^{1/2}Sc^{1/3} \quad (8)$$

By substituting the velocity term in Eq. (8) with the average vibrational velocity over half a cycle ($0.64A\omega$), the time average value of Sh_v can be estimated by,

$$Sh_v = 0.542 Re_v^{1/2}Sc^{1/3} \quad (9)$$

Attempts to use Eqs. (4) and (5) to correlate the experimental data resulted in average deviation in excess of 50%, a fact that is consistent with the finding of Al Taweel and Ismail [17], and Liu et al. [18], where the STFLM approach was found to overemphasize the effect of the amplitude, while the BLTH did not entirely account for its effect. Similarly, an average deviation of 38% was obtained while attempting to correlate the data using Eq. (7), which is close to the observations reported by Liu et al. [18]. However, and as seen from Fig. 6, the entire set of experimental data (107 runs) was satisfactorily correlated (with an average relative error of 8.6%) using the newly developed Eq. (9). This is consistent with the findings of Prasad and Ramanathan [35] in the case of heat transfer, and is very close to the correlation of Liu et al. [18] (a coefficient of 0.54 as compared to 0.52 in their case) who used a copper sulfate/sulfuric acid system and covered a smaller range of experimental conditions (A = 0.57–2.3 mm, f = 13–36 Hz, and L = 12.7–50.8 mm). Figs. 7 and 8 show a comparison between the different model

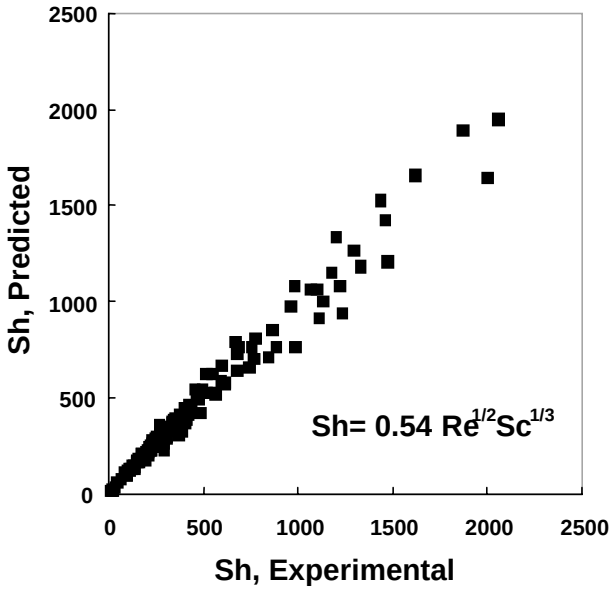

Fig. 6. Correlation of experimental data $Sh_v = 0.54 Re_v^{1/2}Sc^{1/3}$.

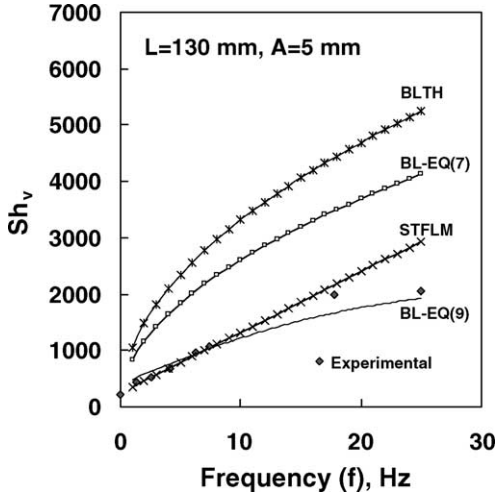

Fig. 7. Comparative evaluation of mass transfer models (L = 130 mm, A = 5 mm).

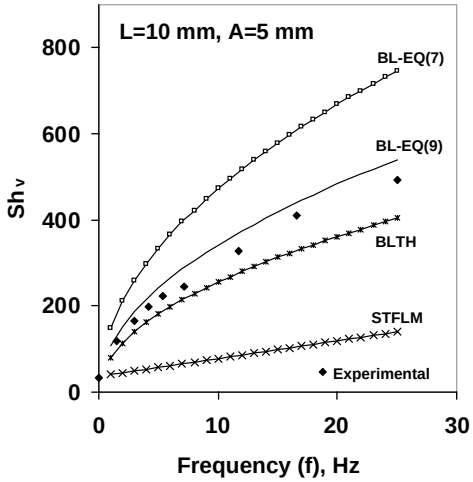

Fig. 8. Comparative evaluation of mass transfer models ($L = 10$ mm, $A = 5$ mm).

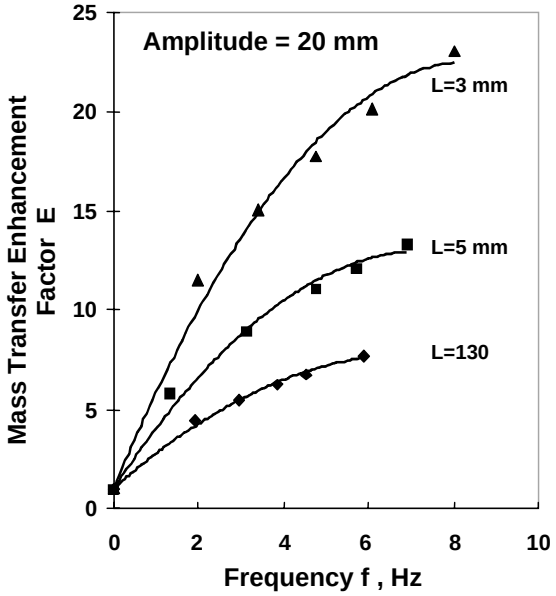

Fig. 9. Effect of vibrational frequency on the mass transfer enhancement factor ($A = 5$ mm).

which clearly demonstrates the suitability of using Eq. (9) for correlating the experimental data. Such a general agreement, however, may only be considered as an empirical approach to allow for predicting the effect of vibration on the average rate of mass transfer. Its major drawback is that it attributes the mass transfer enhancement solely to the increase in relative velocity between the phases as induced by the vibratory motion. The fact that the latter changes direction each cycle does not explain the experimentally observed augmentation of the steady-state mass transfer component. Such discrepancies indicate the need for a more elaborate analysis to satisfactorily explain the mechanism by which transfer rate enhancement is achieved at vertically vibrating surfaces.

3.3. Mass transfer enhancement

The effectiveness of using vibration as a means for enhancing mass transfer may best be expressed by using the mass transfer enhancement factor (E) given by

$$E = \frac{k_v}{k_{nc}} \tag{10}$$

Figs. 9–11 show the effect of vibrational frequency and amplitude on the mass transfer enhancement factor (E) for different electrode heights. As can be seen from those figures, mass transfer enhancement increases with increasing either the frequency or the amplitude of vibration with the extent of enhancement being most pronounced at small electrode heights. For example, under the same vibrational conditions a maximum enhancement factor of about 23 was obtained for electrodes with a 3 mm active height, whereas the corresponding E value is about 8 in the case of electrodes with 130 mm active height. Combining Eqs. (2), (9) and (10), the enhancement factor E can be expressed as,

$$E = 0.81 Re_v^{0.5} Sc^{0.083} Gr^{-0.25} \tag{11}$$

This correlation compares reasonably well with that obtained by Al Taweel et al. [16] with respect to the effect of amplitude (an exponent of 0.5 as compared to 0.42 in their case). On the other hand, their correlation exhibits a much stronger dependence on vibrational frequency (an exponent of 1.09 as compared to 0.5 in our case). This could probably be attributed to the onset of lateral electrode vibrations at its resonant frequency, a factor that would provide additional mass transfer enhancement around the natural

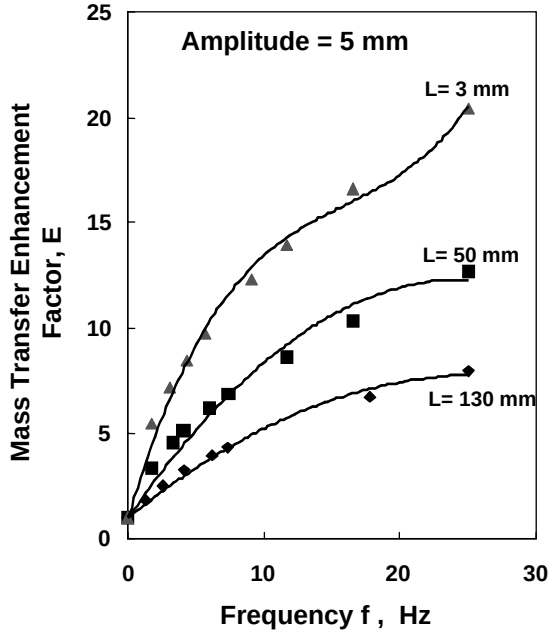

Fig. 10. Effect of vibrational frequency on the mass transfer enhancement factor ($A = 10$ mm).

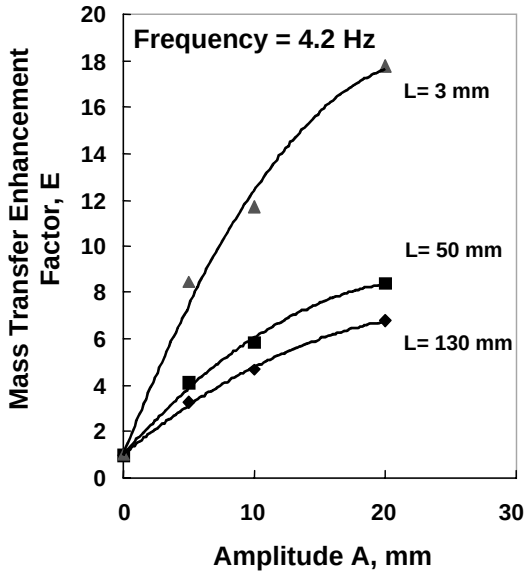

Fig. 11. Effect of vibrational amplitude on the mass transfer enhancement factor ($f = 4.2$ Hz).

resonance frequency. The use of lateral ribs in the present investigation (to eliminate the occurrence of this extraneous and uncontrollable factor) resulted in eliminating this source of error in our experimental results.

4. Conclusions

Based on the above mentioned findings it is possible the reach following conclusions:

- The mass transfer rate at vertical surfaces can be significantly enhanced by longitudinally vibrating them in a direction parallel to their surfaces. The extent of mass transfer enhancement depends on the amplitude and frequency of vibration as well as on the length of the electrode. Up to 23-fold enhancement in the mass transfer was achieved by vibrating short active heights at high vibrational velocities.
- The average mass transfer coefficient at vibrating electrodes can be predicted using the conventional equations of mass transfer over flat surfaces in which a pseudo-steady velocity (equal to the average over one half of the vibration cycle) is utilized.
- The instantaneous value of the mass transfer coefficient was found to be composed of a small oscillatory component superimposed on a large steady one. This suggests that the mass transfer boundary layer is not strongly responsive to the oscillatory velocity. In other words, although the surface velocity periodically approaches zero and reverses direction the mass transfer fluxes undergoes relatively little changes throughout the vibratory cycle, which implies that boundary layer thinning due to vibratory motion plays an important role in this phenomenon.
- Application of vibratory mass transfer enhancement to electrochemical processing results in significant performance improvement. It reduces concentration polarization with the consequent acceleration of metal deposition and dissolution rates and increase of its current efficiencies. It facilitates the formation of fine metallic powder deposits, and the release of bubbles at gas-forming electrodes. It can also results in significant reduction in the volume of the processing units needed for electro-processing purposes, which reduces its overall processing and capital costs.
- More work is necessary to develop a better understanding of the interaction of the different transport mechanisms under vibrating conditions.

References

[1] M.V. Leland, F.R. Alvarez, E.L. Giroux, Reduction of concentration polarization in pervaporation using vibrating membrane module, J. Membr. Sci. 153 (1999) 233–241.
[2] P. Blanpain-Avet, N. Doubrovine, C. Lafforge, M. Laland, The effect of oscillatory flow on crossflow microfiltration of beer in a tubular mineral membrane system, J. Membr. Sci. 152 (1999) 151–174.
[3] R.S. Alasser, H.M. Badr, H.A. Mavromatis, Heat convection from a sphere placed in an oscillating free stream, Int. J. Heat Mass Trans. 42 (1999) 1289–1304.
[4] S. Najarian, B.J. Bellhouse, Effect of oscillatory flow on the performance of a novel cross-flow affinity membrane device, Biotech. Prog. 13 (1997) 113–116.
[5] M.R. Mackley, P. Stonestreet, Heat transfer and associated energy dissipation for oscillatory flow in baffled tubes, Chem. Eng. Sci. 50 (1995) 2211–2224.
[6] M.R. Hewgill, M.R. Mackley, A.B. Pandit, S.S. Pannu, Enhancement of gas–liquid mass transfer using oscillatory flow in baffled tube, Chem. Eng. Sci. 48 (1993) 799–809.
[7] W.L. Cooper, K.T. Yang, V.W. Nee, Fluid mechanics of oscillatory and modulated flows and associated applications in heat and mass transfer—a review, J. Energy Heat Mass Transfer 15 (1993) 1–19.
[8] M.R. Mackley, G.M. Tweedle, I.D. Wyatt, Experimental heat transfer measurements for pulsatile flow in baffled tubes, Chem. Eng. Sci. 45 (1990) 1237–1242.
[9] A.M. Al Taweel, J. Landau, Effect of oscillatory motion on mass transfer between a solid sphere and fluids, Can. J. Chem. Eng. 54 (1976) 532–540.
[10] P.D. Richardson, Effect of sound and vibrations on heat transfer, Appl. Mech. Rev. 20 (1967) 201–217.
[11] F. Marken, et al., Electrolysis in the presence of ultrasound: cell geometries for the application of extreme rates of mass transfer, J. Chem. Soc., Perkin Trans. 2 (1997) 2055–2059.
[12] P. Cognet, J. Berlan, G. Lacoste, P. Fabre, M. Jud, Application of metallic foams in an electrochemical pulsed flow reactor I: mass transfer performance, J. Appl. Electrochem. 25 (1995) 1105–1112.
[13] G.H. Sedahmmed, M.Z. El-Abd, A.A. Zatout, Y.A. El-Taweel, M.M. Zaki, Mass transfer behavior of electrochemical reactors employing vibrating screen electrodes, J. Electrochem. Soc. 141 (1994) 437–440.
[14] M.M. Zaki, Y.A. El-Taweel, A.A. Zatout, M.Z. El-Abd, G.H. Sedahmmed, Mass transfer at oscillating grids, J. Electrochem. Soc. 138 (1991) 430–434.
[15] A. Ratel, P. Duverneuil, G. Lacoste, Influence de la pulsation liquide sur le comportement d'un reacteur Electrochimique Constitue par un lit de Particules Conductrices, I. Transfert de Matiere, J. Appl. Eelectrochem. 18 (1988) 394–400.

[16] A.M. Al-Taweel, M.I. Ismail, M.Z. El-Abd, Effect of vibrations on the mass transfer at vibrating electrodes, Chemie-Ingenier-Technik 46 (1974) 861.
[17] A.M. Al Taweel, M.I. Ismail, Comparative analysis of mass transfer at vibrating electrodes, J. Appl. Electrochem. 6 (1976) 559–564.
[18] M.B. Liu, E.M. Rudnick, G.M. Cook, N.P. Yao, Mass transfer at longitudinally vibrating vertical electrodes, J. Electrochem. Soc. 129 (1982) 1955–1959.
[19] M.B. Liu, G.M. Cook, N.P. Yao, Vibrating zinc electrodes in Ni/Zn batteries, J. Electrochem. Soc. 129 (1982) 913–920.
[20] D.E. Rice, D. Sundstrom, M.F. McEachern, L.A. Klumb, J.B. Talbot, Copper electrodeposition studies with a reciprocating paddle, J. Electrochem. Soc. 135 (1982) 2777–2781.
[21] A. Mahito, T. Nonaka, Ultrasonic effects on electro-organic processes. Part 7. Reduction of benzaldehydes on ultrasound vibrating electrodes, J. Electroanal. Chem. 425 (1997) 161–166.
[22] A. Mahito, T. Nonaka, Ultrasonic effects on electro-organic processes. Electroreduction of benzaldehydes on ultrasound vibrating electrodes, Chem. Lett. (1995) 669–670.
[23] U. Landau, Electro-chemical deposition system and method of electroplating on substrates, US Patent 6,2621,433 (July 2001).
[24] R. Omasa, Plating Method, US Patent 6,2621,435 (July 2001).
[25] P.C. Andricacos, Vertical Paddle Plating Cell, US Patent 5,516,412 (May 1996).
[26] F.G. Bark, S. Zahria, Turbulent free convection in large electro-chemical cells with a binary electrolyte, J. Appl. Eelectrochem. 29 (1999) 27–34.
[27] N.G. Carpenter, E.P.L. Roberts, Mass transport and residence time characteristics of an oscillatory flow electrochemical reactor, Trans. IChemE 77 (A) (1999) 212–217.
[28] C.K. Drummond, F.A. Lyman, Mass transfer from a sphere in an oscillating flow with zero mean velocity, Comput. Mech. 6 (1990) 315–326.
[29] K.S. Rao, G.J.V.J. Raju, C.V. Rao, Indian J. Technol. 3 (1964) 35.
[30] C.V. Rama Raju, A. Ramalinga Sastry, G.J.V.J. Raju, Ionic mass transfer at vibrating plates, Indian J. Technol. 7 (1969) 35–38.
[31] M.G. Fouad, T. Gouda, Natural convection mass transfer at vertical electrodes, Electrochim. Acta 9 (1964) 1071–1076.
[32] J.L. Taylor, T. Hanratty, Influence of natural convection on mass transfer rates for the electrolysis of ferricyanide ions, Electrochim. Acta 19 (1974) 529–533.
[33] J.R. Selman, J. Newman, Free convective mass transfer with a supporting electrolyte, J. Electrochem. Soc. 118 (1971) 1070–1078.
[34] C.B. Watkins, I.H. Herron, Laminar shear layer due to a thin flat plate oscillating with zero mean velocity, Trans. ASME J. Fluids Eng. 100 (1976) 367–373.
[35] K.K. Prasad, V. Ramanathan, Heat transfer by free convection from a longitudinally vibrating vertical plate, Int. J. Heat Mass Transfer 15 (1972) 1213–1223.
[36] A. Acrivos, Combined laminar free- and forced-convection heat transfer in external flows, AIChEJ 4 (1958) 285–289.
[37] H. Schlichiting, Boundary-Layer Theory, seventh ed., McGraw-Hill, New York, 1979, p. 93.
[38] H. Schlichiting, Boundary-Layer Theory, seventh ed., McGraw-Hill, New York, 1979, p. 291.